Journal of Metals, Materials and Minerals, 35(2), e2232, 2025

Photocatalytic behaviour of $(BiYbO_3)_{0.5}$-$(BaTiO_3)_{0.5}$

Yasaswi Priyadarshini SAMAL[1], Subhalaxmi PATRA[1], Tapan DAS[1], and Minakshi PADHY[1,*]

[1]*Department of Chemistry, NIIS Institute of Information Science and Management (Degree) College, Sarada Vihar, Bhubaneswar- 752054 India*

***Corresponding author e-mail**: moon.94371@gmail.com

Received date:
17 December 2024
Revised date:
4 January 2025
Accepted date:
4 April 2025

Keywords:
Rare earth;
Nanomaterial;
Photocatalyst;
Malachite green

Abstract

Different organic compounds like dyes and pharmaceutical contaminants pollute a large amount of water which can increase the chemical oxygen demand in water bodies. The photodegradation of dyes has been widely studied using TiO_2-based nanomaterials, which are typical photocatalysts. TiO_2 is highly effective in reducing pollutants when exposed to UV light and does not cause secondary pollution. However, TiO_2 is only functional when exposed to UV light, which is not ideal for real-world use. This drawback of TiO_2 pulls the research towards modified photocatalysts for better yield. In this study, the $(BiYbO_3)_{0.5}$-$(BaTiO_3)_{0.5}$ material was formulated by solid state reaction technique. This material is crystallized to Tetragonal, P4mm. The nano-rod structure can be observed from the FESEM. The photo degradation behavior of the material is observed against the pollutant i.e. Malachite Green. It is found that the photocatalytic degradation of Malachite green is 92.2% in 60 min.

1. Introduction

The lead free ferroelectric perovskites like $BaTiO_3$, $KNbO_3$, $Bi_{0.5}Na_{0.5}TiO_3$, $BiFeO_3$ are studied extremely because of their wonderful properties i.e. ferroelectric, dielectric, optical and others [1]. Altering the chemical compositions of $BaTiO_3$ by doping other elements, it appears that the physical properties are drastically changed. Due consideration is now being given to the trivalent rare-earth (R-E) ions for their extraordinary capacity to modify the electrical properties of $BaTiO_3$ [2-5]. The intermediate sized R-E ions like Ho^{3+}, Eu^{3+}, Gd^{3+} and Dy^{3+}, in particular, are more companionable for switch at A-site as well as B-site of a perovskite. This kind of behavior is known as self-compensation system. The occupancy of the R-E ions in A/or B positions, however, is extremely reliant on the thermodynamic and physical-experimental states [6]. When doped with $BaTiO_3$, the smaller rare-earth ions, such as Yb^{3+} and Lu^{3+}, are in the B-site, while the bigger ions, such as Lanthanum ion (La^{3+}) and Cerium ion (Ce^{3+}), are at the A-site [6]. When it diffuses in the A-site and B-site, the rare-earth element takes on the roles of a donor and an acceptor, respectively. The amphoteric nature of R-E ions maintains the equilibrium among donor-acceptor, increasing the material's dependability. Due to its intriguing characteristics, such as non-toxicity, high thermal stability, optical transmittance behaviors, and photo-luminescence capabilities, attention to rare earth doped nano-composites is growing daily [7,8]. In comparison to luminous materials based on sulphide, R-E co-doped strontium aluminate exhibits superior phosphorescence, efficient quantum yield, and stable chemical behaviors [8].

The positive temperature coefficient of resistance (PTCR) behavior of polycrystalline $BaTiO_3$ is increased by adding small amounts of Bi^{3+} at Ba-sites, while also restricting grain development. Lowering the sintering temperature of $BaTiO_3$ and maintaining complete tetragonality in $BaTiO_3$ ceramic are two additional benefits of Bi^{3+} doping [9]. This can be observed from the literature that Yb and Bi based materials like $BiYbO_3$ has lower dielectric loss with decent relative permittivity. In addition, the material exhibits significant grain boundary resistivity (i.e., $8.256 \times 10^{+7}$) at 25°C, which is indicative of negative temperature coefficient of resistance (NTCR) nature. Additionally, high efficacy of energy storage for (1-x)$BaTiO_3$-x$BiYbO_3$ compounds were analyzed extensively. $BaTiO_3$ has good electro-optical performance and broad band gap energy (4.3 eV to 3.27 eV). Additionally, it possesses relatively superior solid-solubility for a variety of R-E activators (cations like: Ce^{3+}, Nd^{3+}, Sm^{3+}, Eu^{3+}, Gd^{3+}, Dy^{3+}, Ho^{3+}, and Er^{3+}). The utilization of Re-ions functions as an excellent alternative in NIR-to-visible ceramic oxides, especially in fluorescent applications. This has been reported that the allowed optical band gap for $Bi_{0.5}Ba_{0.5}Yb_{0.5}Ti_{0.5}O_3$ is 1.75 eV (for direct) and 1.41 eV (for indirect) [10].

A type of triphenylmethane dye known as Malachite Green (MG) is used comprehensively in the production of pottery, leather, textiles, food coloring, cell coloring, etc. Due to its high level of disinfection effectiveness, it is also employed in the aquaculture sector to cure fish body scratches and prevent bacterial infections. MG and its reduced variants, however, have been discovered by researchers to be extremely poisonous, persistent, carcinogenic, and mutagenic [11].

Many efforts have been made recently to use photocatalysis to get rid of organic dyes (Malachite Green (MG) in contaminated water [12,13]. The photodegradation of dyes has been widely studied using TiO_2-based nanomaterials, which are typical photocatalysts [14,15]. TiO_2 is highly effective in reducing pollutants when exposed to UV light and does not cause secondary pollution. However, TiO_2 is only functional when exposed to UV light, which is not ideal for real-world use [16,17]. Significant research has been done in the last few decades to increase the photocatalysis process' effectiveness. Charge-separation

techniques are intentionally implemented to limit the recombination of electrons and holes since photo-induced electron-hole couples have a relatively short lifetime due to the recombination process [18].

In this study, the $(BiYbO_3)_{0.5}$-$(BaTiO_3)_{0.5}$ (BYBTO) material is synthesized, after that the structural, morphological, and photocatalytic study of the materials are done by taking Malachite Green.

2. Experimental study

2.1 Formulation of $(BiYbO_3)_{0.5}$-$(BaTiO_3)_{0.5}$

The synthesis of the material BYBTO was executed by adopting the commercial solid-state-reaction method. Both the compounds were prepared by taking high clarity oxides (Mis Loba Chemie Pvt. Ltd., India) and carbonates (Mis Chemical Drug House) in a stoichiometry proportion i.e. Bi_2O_3, TiO_2, $BaCO_3$ and Yb_2O_3. The stoichiometric quantity of required oxides/carbonates was blended by taking dry chemicals for 1 h. After that, methanol was added in the above mixture for wet grinding. The wet grinding process was done for 4 h to obtain a homogeneous mixer. The prepared mixer was calcined at 950°C (12 h) in covered high purity alumina crucible. After that the preliminary structural phase of the calcined material was studied by XRD (X-ray diffraction). After the conformity of the aspired crystal structure, pellets were done through mixing 1% of PVA (binder) with the powder of the BYBTO. For the pellet formation KBr-hydraulic press (pressure = 4×10^6 kg·m^{-2}) was used. Then the sintering of cylindrical pellets was done at 1000°C. These pellets are used to analyze different behaviors like surface morphology, UV-DRS, etc. The powder form of the material was utilized to study photo catalytic behavior of the materials.

The sintered pellets were polished with fine sandpaper to provide a parallel and a flat surface before being used for further research. A 5 keV electron beam (Model-SIGMA ZEISS) and in-lens detector were used in FESEM (Field emission scanning electron microscopy) to capture the surface morphology of the material. A diffused reflectance setup fastened to a UV-VIS-NIR spectrometer (Agilent carries 5000 UV-Vis-NIR) was used to capture the absorption spectra of various materials. For the examined material, the spectra were gathered in the 300 nm to 800 nm wavelength range.

2.2 Photo-catalytic experiment of synthesized materials

The photo-degradation experiment was done by taking the material BYBTO as catalysts. The Photo-degradation of MG has been accomplished by taking 20 mL of 200 mg·L^{-1} freshly made MG solutions with 1 g·L^{-1} of catalyst. The entire photocatalytic degradation was done in Odisha (Bhubaneswar), at a standard sunshine illumination of 100,000 lux for 60 min in between 12 a.m. to 1 p.m. To maintain the pH at 5, 0.1 M HCl, and 0.1 M NH_4OH solution were added to the mixture. Because the dye can be degraded more effectively by the hydroxyl radical than the hole, this predominates in the alkaline state [19]. The solution was initially stored in the dark-place for 10 min to attain the adsorption-desorption equilibrium and then placed under sunshine illumination. After degradation the catalyst and the concentration of the MG were separated from the suspension using centrifugation. The UV-visible spectrophotometer (JASCO 750) was used to calculate the amount of MG left after photocatalytic degradation. The photocatalytic efficiency can be calculated as follows:

$$\eta = \frac{(C_0 - C_t)}{C_o} \times 100 \quad (1)$$

Where, C_0 and C_t represent the intial-concentration and concentration at time t of the solution, respectively.

The production of an electron-hole pair (e^-/h^+) subsequently proceeds to the catalyst's surface and undergoes redox reaction through the molecules attached with it. It happens when light strikes a semiconductor by the energy equivalent to or more than the semi-conductor's band gap.

The molecules of H_2O are oxidized by the h^+ (holes) to create hydroxy-radicals ($OH^\bullet$). The e^- (electrons) produce $O_2^{-\bullet}$ i.e. superoxide radical anion of oxygen from the dissolved oxygen.

$$\text{Photocatalyst} + h\nu \rightarrow h^+ + e^- \quad (2)$$

$$H_2O + h^+ \rightarrow OH^\bullet + H^+ \quad (3)$$

$$O_2 + e^- \rightarrow O_2^{-\bullet} \quad (4)$$

The dye is decolorized as a result of the production of $O_2^{-\bullet}$ and $OH^\bullet$. The dye molecules are oxidised and generate different simplex species. More $OH^\bullet$ are formed through the reaction of the superoxide-radical anions and H^+ ions which helps to oxidize the dye. The entire photocatalytic process is depicted in Figure 1.

$$OH^\bullet + \text{dye} \rightarrow \text{Dye degradation} \quad (5)$$

$$O_2^{-\bullet} + \text{dye} \rightarrow \text{Dye degradation} \quad (6)$$

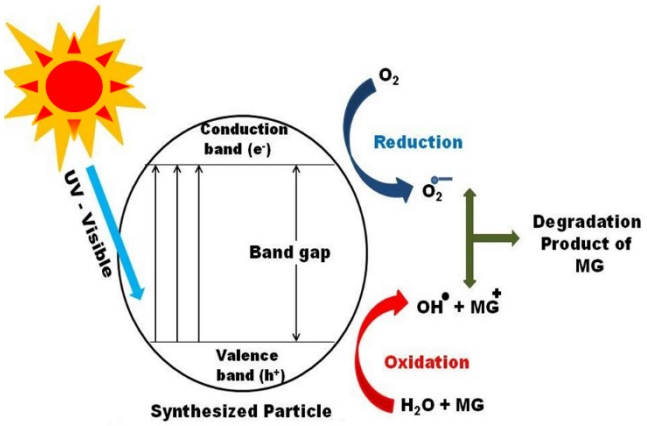

Figure 1. Photocatalytic mechanism.

3. Result and discussion

3.1 Study of XRD and FESEM

The XRD of BYBTO was studied with the help of X'pert Highscore Plus. It is observed that the XRD peaks are approximately same with the reference material $BaTiO_3$ (ICSD code-027965), which has P4mm tetragonal structure and lattice constants a = b = 3.98 Å, c = 4.01 Å,

$\alpha = \beta = \Upsilon = 90°$. From this observation the tetragonal-P4mm structure of BYBTO is considered. The high intense peaks at 22.38°, 31.48°, 31.62°, 39.08°, 45.1°, 45.40°, 50.08°, 50.64°, 56.60°, 66.34°, 70.0°, 75.26°, 79.16° etc. are matched with the reference material $BaTiO_3$. The peaks of XRD suggest the tetragonal phase (P4mm-99) of the material BYBTO. Except these peaks other peaks are also observed at 28.56°, 30.98°, and 57.52° that shows a very few small minor phases (like $BiYbO_3$, $YbTiO_3$, $Bi_4Ti_3O_{12}$, marked with * in Figure 2).

The crystallite size of the synthesized compound is evaluated by applying Scherer relation, $D_{hkl} = K\lambda/\beta_{0.5}Cos\theta$, here K= 0.89, λ is equivalent to 1.5418 Å, $\beta_{0.5}$ is the peak breadth at half maximum "FWHM" [20]. The crystallite-size of BYBTO is found be 77.60 nm. FESEM of BYBTO is represented in Figure 3. In FESEM image it can be observed that many of the particles/ grains are needle shaped.

3.2 UV-Vis study

The UV-visible-DRS for BYBTO is provided in Figure 4(a). The maximum absorbance peak for BYBTO is observed at 395 nm. The band gap (optical) is calculated from Tauc's equation as below:

$$\alpha h\nu = A\left(h\nu - E_g\right)^n;\ \alpha = 2.303\ A/t \qquad (7)$$

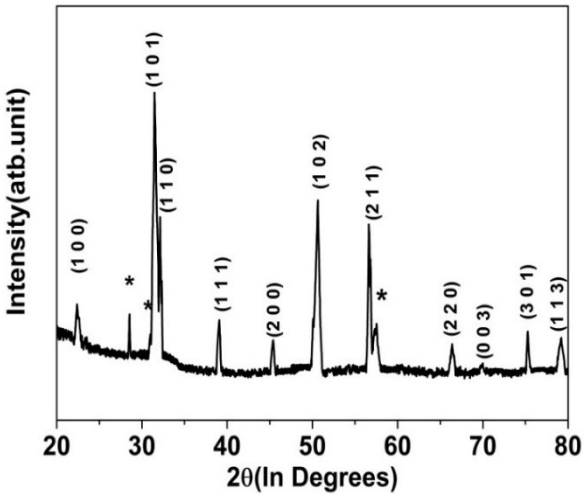

Figure 2. XRD of BYBTO.

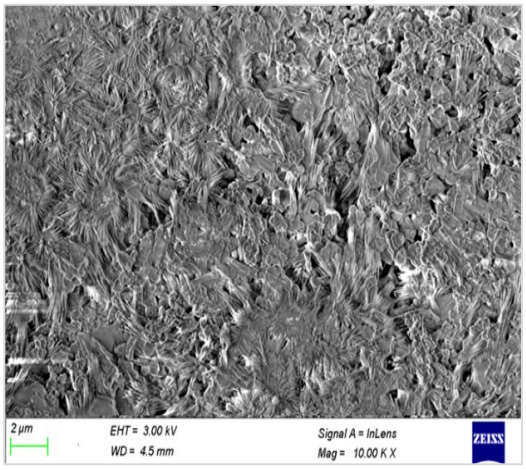

Figure 3. FESEM of BYBTO.

Here, A = optical invariable, α = absorption-coefficient, E_g = optical band gap, and t = thickness of the material. The value of n (transition dependent index) is 1/2 and 2 for direct and indirect allowed transitions, respectively [21]. The direct allowed transition optical band gap for BYBTO is calculated as 1.86 eV (Figure 4(b)).

3.4 Photocatalytic activity

In this study, the synthesized material BYBTO is used as a catalyst for photo-degradation of 200 ppm MG solution. The photo degradation of MG was completed by mixing 0.02 g of catalyst to 20 mL of the MG solution. Initially, the pH of the solution was kept to 5 by adding 0.1 M HCl and 0.1 M NH_4OH solution; because the literature study shows that $10 \leq pH \leq 5$ lower the degradation rate [22]. At first the catalyst mixed solution was kept in the dark for 10 min to obtain the adsorption–desorption equilibrium. Then the process is followed by exposing the solution-mixture under sunshine illumination for 60 min to analyze the photo-degradation property. The absorption-spectrum of all the catalysts was noticed in the wavelength range of 450 nm to 700 nm at various time intervals. The main absorption peak of these catalysts was noticed at 614 nm.

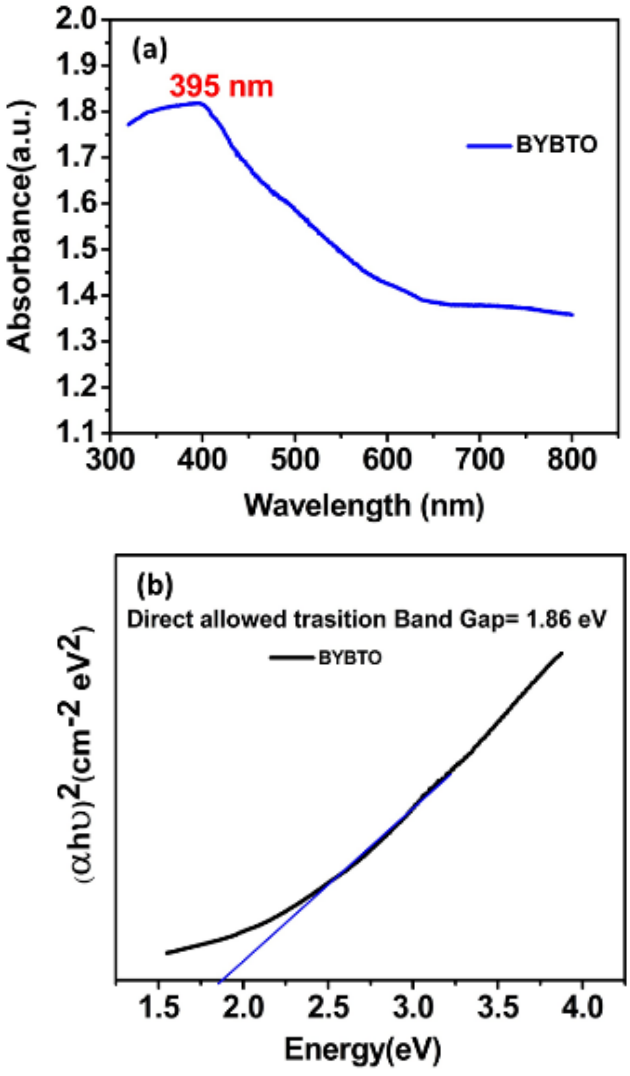

Figure 4. (a) UV-Vis (DRS), and (b) Tauc's plot for BYBTO.

The experiment was done by adding 0.02 g of catalyst in 200 ppm MG solution at pH 5. This experiment was conducted for 60 min. The Photo-degradation of MG solution by adding catalyst BYBTO is shown in Figure 5(a). Primarily, photolysis-reaction has been progressed in presence of sun-light without the addition of photocatalyst. It is observed that a smaller amount of MG has been degraded. Further, the experiment has been progressed by adding a catalyst without light for 30 min. It has been seen that some amount of MG is adsorbed on the active sites of the catalyst. The MG adsorption-percentage has been documented as 31%. At last the study of photocatalysis has been done in presence of sunlight irradiation.

Throughout the sunlight irradiation experiment, electrons (e^-) are driven out from VB (Valence Band) to CB (Conduction Band) and generated photo-excited e^- in CB and h^+ in VB. At the same time the photo-excited h^+ moves to the surface and react with H_2O to produce $OH^\bullet$. Whereas the released photo-electrons (in CB) is responsible for reducing the O_2 molecules present on the surface of catalyst and/or dissolved in solution to the $O_2^{-\bullet}$. These radicals ($OH^\bullet$ and $O_2^{-\bullet}$) are involved in the degradation of Malachite Green. Table 1 gives the studied photocatalytic degradation (%) of BYBTO at 10 min, 30 min, and 60 min.

3.4.1 Kinetic analysis

The kinetic study of photodegradation of MG process over BYBTO was observed in 10 min interval of time (from 10 min to 60 min). From the graph (Figure 5(b)) it can be seen that the photo-degradation of MG pursued the 1st order reaction kinetics for all catalysts.

$$\log\frac{C_0}{C} = \frac{K_t}{2.303} \quad (8)$$

$$K = \log\frac{C_0}{C} \times \frac{2.303}{t} \quad (9)$$

Here, first-order rate constant is K, C_0 is the initial concentration of MG and C is the concentration at time t. The slope-intercept equation for linear line BYBTO is given in Figure 5(b). The K value of MG reduction on BYBTO at specified time is presented in Table 2.

3.4.2 The photocatalytic reaction mechanism of BYBTO

The electrons in barium do not participate in the VB and CB, while it provides electrons to equilibrium the charge in the system. Hence, the band gap value of $BaTiO_3$ relies on the relative energy positions of the Ti-3d and O-2p states and absorption occurs in UV region.

The band positions for the above synthesized material, i.e. $BiYbO_3$ [23], BYBTO were estimated as below:

$$E_{VB} = X - E_C + 0.5E_g \quad (10)$$

Here E_{VB} is potential of VB, E_C is ~4.5 eV (free electron energy on SHE standard hydrogen scale), Eg is optical band gap, and X is the electronegativity of the semiconductor [24]. The potential of CB (E_{CB}) can be determined by the following Equation (11):

$$E_g = E_{VB} - E_{CB} \quad (11)$$

Table 3 shows the optical band gap, valance band potential, and conduction band potential for pure ($BiYbO_3$, $BaTiO_3$) particles and BYBTO material. Figure 6 demonstrates the diagram of the band structure for undoped $BaTiO_3$ and BYBTO. From the schematic illustration, it can be seen that the optical band gap reduced in BYBTO as compared to pure $BaTiO_3$.

Due to the stability, low-cost and the wide light response properties of Bi, Bi is doped in other materials like TiO_2 to enhance the photo-catalytic performance of the material efficiently [26].

The behaviors of Bi_2O_3 as an electron-conducting material (Bi-6p) and intrinsic polarizabilities (Bi-6s lone electron-pairs), promote the dissociation of photogenerated e^-- h^+ pairs and the transference of the charge-carrier(s) [26].

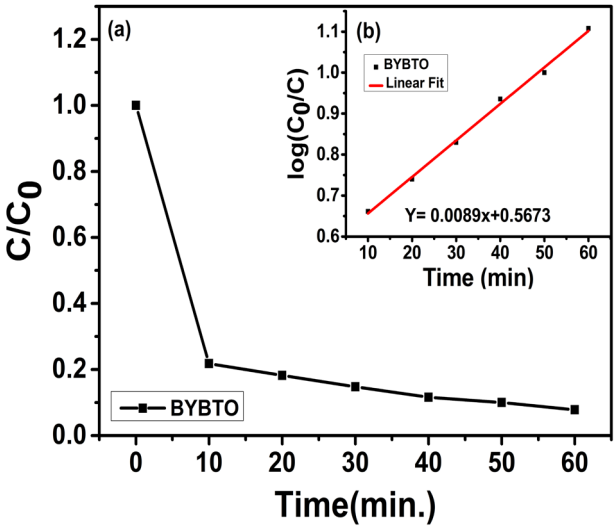

Figure 5. (a) Photo-degradation, (b) kinetic study of photodegradation of MG process over BYBTO kinetic study of photodegradation of MG process over BYBTO.

Table 1. The photo-degradation (%) of BYBTO at 10 min, 30 min, and 60 min.

Time [min]	Photo-degradation [%]
10	78.2
30	85.2
60	92.2

Table 2. The K value of MG reduction on BYBTO at specified time.

Log C_0/C					
10 min	**20 min**	**30 min**	**40 min**	**50 min**	**60 min**
0.66154	0.73993	0.82974	0.93554	1.00000	1.10791

Table 3. The optical band gap (Eg), valance band potential (E_{VB}), and conduction band potential (E_{CB}) for pure ($BiYbO_3$, $BaTiO_3$) particles and modified particle (synthesized) BYBTO.

Materials	Eg [eV]	E_{VB} [eV]	E_{CB} [eV]
$BiYbO_3$ [23]	2.20	2.27	0.07
$BaTiO_3$ [25]	3.03	2.88	- 0.15
BYBTO	1.75	1.46	-0.29

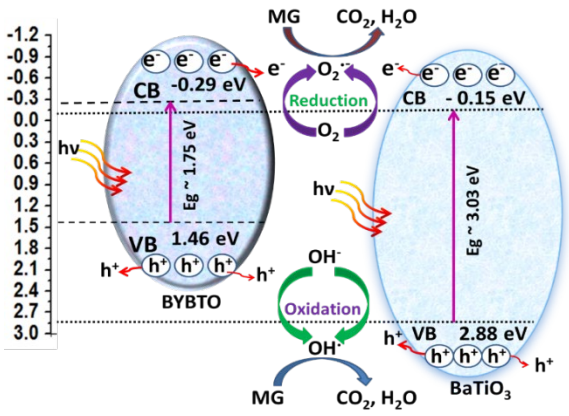

Figure 6. The scheme of band positions for $BaTiO_3$ and BYBTO particles.

Yb^{3+} doped TiO_2 can create electron capture centers, facilitating the separation of pairs of electrons and holes. This was explained by the creation of an empty 4f impurity energy level in the rare earth ions in the TiO_2 energy band structure between the conduction and valence bands [27]. The formation of internal band due to doping of Yb and Bi species in $BaTiO_3$ will excite the electron in the valence band of that material under visible light. Bi^{3+} and Yb^{3+} react with electron acceptors like O_2 adsorbed on the catalyst surface or dissolved in solution to $O_2^{-\bullet}$ and reduce the excited electron.

In the meantime, the hole(s) in $BaTiO_3$'s valence band reacts with H_2O to produce $OH^{\bullet}$, and $O_2^{-\bullet}$. These produced extremely potent oxidizing-agents can then oxidize the MG to produce breakdown particles. In contrast, when exposed to UV light, the electron is energized to move into the conduction band of the $BaTiO_3$ material and subsequently leaps to the internal band made up of the elements Bi and Yb. The formed O_2 is subsequently transferred to the O_2 that has been adsorbed on the catalyst surface. Water molecules and the valence band's holes combine to create an $OH^{\bullet}$ radical. The MG is oxidized by the resultant $O_2^{-\bullet}$ and $OH^{\bullet}$ to produce CO_2 and H_2O as breakdown byproducts.

4. Conclusion

The synthesis of BYBTO material was done by using the conventional solid state technique. The photocatalytic degradation of Malachite Green is observed by taking the above synthesized material. The nano-rod structure can be observed from the FESEM. It is found that the photocatalytic degradation of Malachite green is 92.2% in 60 min after using BYBTO photocatalyst.

Conflict of Interest

The authors declare that they have no conflict of interest.

Acknowledgements

The authors would like to give their sincere thanks to Dr. P. Ganga Raju Achary, Department of Chemistry, Siksha 'O' Anusandhan, Deemed to be University, and Dr. Pratap Kumar Sahoo, Department of Physics, National Institute of Science Education and Research (NISER) of Bhubaneswar for their kind support.

Reference

[1] T. Badapanda, V. Senthil, S. Panigrahi, and S. Anwar, "Diffuse phase transition behavior of dysprosium doped barium titanate ceramic," *Journal of Electroceramics*, vol. 31, no. 1-2, pp. 55-60, 2013.

[2] A. Kumari, A. Vij, Mohd. Hashim, A. Dubey, and S. Kumar, "Enhancement in the dielectric properties of Sm doped $BaTiO_3$ bulk ceramics," presented at the The 3rd Joint International Conference On Energy Engineering And Smart Materials (Iceesm-2018) And International Conference On Nanotechnology And Nanomaterials In Energy (ICNNE-2018), Milan, Italy, 2018, p. 030012.

[3] M. Ganguly, S. K. Rout, W. S. Woo, C. W. Ahn, and I. W. Kim, "Characterization of A-site deficient samarium doped barium titanate," *Physica B: Condensed Matter*, vol. 411, pp. 26-34, 2013.

[4] Z.Yao, H. Liu, Y. Liu, Z. Wu, Z. Shen, Y. Liu, and M. Cao, "Structure and dielectric behavior of Nd-doped $BaTiO_3$ perovskites," *Materials Chemistry and Physics*, vol. 109, no. 2-3, pp. 475-481, 2008.

[5] M. Ganguly, S. K. Rout, T. P. Sinha, S. K. Sharma, H. Y. Park, C. W. Ahn, and I. W. Kim, "Characterization and rietveld refinement of A-site deficient lanthanum doped barium titanate," *Journal of Alloys and Compounds*, vol. 579, pp. 473-484, 2013.

[6] Y. A. Zulueta, T. C. Lim, and J. A. Dawson, "Defect clustering in rare-earth-doped $BaTiO_3$ and $SrTiO_3$ and its influence on dopant incorporation," *Journal of Physical Chemistry C*, vol. 121, no. 42, pp. 23642-23648, 2017.

[7] M. M. S. Sanad, M. M. Rashad, E. A. Abdel-Aal, M. F. El-Shahat, and K. Powers, "Optical and electrical properties of Y^{3+} ion substituted orthorhombic mullite $Y_{(x)}Al_{(6-x)}$ Si_2O_{13} nanoparticles," *Journal of Materials Science: Materials in Electronics,* vol. 25, no. 6, pp. 2487-2493, 2014.

[8] M. Padhy, R. N. P. Choudhary, and P. G. R. Achary, "Effect of Bi and Sm ion doping in barium titanate ceramic: Dielectric, optical and ferroelectric study," *Applied Physics A* , vol. 127, no. 11, p. 847, 2021.

[9] P. Padmini, and T. R. N. Kutty, "Influence of Bi^{3+} ions in enhancing the magnitude of positive temperature coefficients of resistance in n-$BaTiO_3$ ceramics," *Journal of Materials Science: Materials in Electronics*, vol. 5, no. 4, 1994.

[10] M. Padhy, S. A. Behera, R. N. P. Choudhary, and P. G. R. Achary, "Studies of structure, dielectric and conduction mechanism of Bi^{3+}/Yb^{3+} modified $BaTiO_3$," *Journal of the Indian Chemical Society*, vol. 99, no. 8, p. 100591, 2022.

[11] K. V. K. Rao, "Inhibition of DNA synthesis in primary rat hepatocyte cultures by malachite green: a new liver tumor promoter," *Toxicology Letters*, vol. 81, no. 2-3, pp. 107-113, 1995.

[12] A. Fujishima, T. N. Rao, and D. A. Tryk, "Titanium dioxide photocatalysis," *Journal of Photochemistry and Photobiology C: Photochemistry Reviews,* vol. 1, no. 1, pp. 1-21, 2000.

[13] M. A. Fox, and M. T. Dulay, "Heterogeneous photocatalysis," *Journal of chemical reviews*, vol. 93, no. 1, pp. 341-357, 1993.

[14] Y. Chen, Y. Zhang, C. Liu, A. Lu, and W. Zhang, "Photo-degradation of malachite green by nanostructured BiWO visible light-induced photocatalyst," *International Journal of Photoenergy*, vol. 2012, pp. 1-6, 2012.

[15] Y. Q. Wang, X. J. Yu, and D. Z. Sun, "Synthesis, characterization, and photocatalytic activity of TiO_2−xNx nanocatalyst," *Journal of Hazardous Materials*, vol. 144, no. 1-2, pp. 328-333, 2007.

[16] R. Asahi, T. Morikawa, T. Ohwaki, K. Aoki, and Y. Taga, "Visible-light photocatalysis in nitrogen-doped titanium oxides," *Science*, vol. 293, no. 5528, pp. 269-271, 2001.

[17] J. C. Yu, L. Zhang, Z. Zheng, and J. Zhao, "Synthesis and characterization of phosphated mesoporous titanium dioxide with high photocatalytic activity," *Chemistry of Materials*, vol. 15, no. 11, pp. 2280-2286, 2003.

[18] R. M. Pallares, X. Su, S. H. Lim, and N. T. K. Thanh, "Fine-tuning of gold nanorod dimensions and plasmonic properties using the Hofmeister effects," *Journal of Materials Chemistry C*, vol. 4, no. 1, pp. 53-61, 2016.

[19] E. M. M. Putri, M. Rachimoellah, C. S. Rahendaputri, Y. Adisti, and Y. Zetra, "Photocatalytic degradation of malachite green using TiO_2 and O_2/UV," presented at the The 3rd International Seminar On Chemistry: Green chemistry and its Role for Sustainability, Surabaya, Indonesia, 2018, p. 020092.

[20] P. G. R. Achary, S. K. Dehury, and R. N. P. Choudhary, "Structural, electrical and dielectric properties of double perovskites: $BiHoZnZrO_6$ and $BiHoCuTiO_6$," *Journal of Materials Science: Materials in Electronics*, vol. 29, no. 8, pp. 680-6816, 2018.

[21] M. M. S. Sanad, M. M. Rashad, and A. Y. Shenouda, "Novel CuInGaTe structures for high efficiency photo-electrochemical solar cells," *International Journal of Electrochemical Science*, vol. 11, no. 6, pp. 4337-4351, 2016.

[22] K. M. Reza, A. Kurny, and F. Gulshan, "Parameters affecting the photocatalytic degradation of dyes using TiO_2: A review," *Applied Water Science*, vol. 7, no. 4, pp. 1569-1578, 2017.

[23] M. Padhy, R. N. P. Choudhary, and P. G. R. Achary, "Impedance and electrical evaluation of rare earth-based perovskite: $BiYbO_3$," *SPIN*, vol. 11, no. 04, p. 2150019, 2021.

[24] P. R. B, H. Cui, C. S. M, S. V. P. Vattikuti, Y. Suh, and S.-H. Park, "Influence of Gd doping on the visible-light photocatalytic activity and magnetic properties of $BiFeO_3$ particles," *Materials Research Express*, vol. 6, no. 11, p. 115044, 2019.

[25] L. G. Devi, and P. M. Nithya, "Preparation, characterization and photocatalytic activity of $BaTiF_6$ and $BaTiO_3$: A comparative study," *Journal of Environmental Chemical Engineering*, vol. 6, no. 3, pp. 3565-3573, 2018.

[26] H. Xiang, B. Tuo, J. Tian, K. Hu, J. Wang, J. Cheng, and Y. Tang, "Preparation and photocatalytic properties of Bi-doped TiO_2/montmorillonite composite," *Optical Materials*, vol. 117, p. 111137, 2021.

[27] J. Yu, Y. Yang , R. Fan, H. Zhang, L. Li, L. Wei, Y. Shi, K. Pan, and H. Fu, "Er^{3+} and Yb^{3+} co-doped TiO_2−F up-conversion luminescence powder as a light scattering layer with enhanced performance in dye sensitized solar cells," *Journal of Power Sources*, vol. 243, 2013.